Echocardiographic and Hemodynamic Data

	Non-Tg		BNP-Tg	
	Sham	MI	Sham	MI
Echocardiographic data				
LV EDD, mm	4.4±0.1	4.8±0.1†§	4.3±0.1	4.8±0.1*§
LV ESD, mm	3.2±0.2	3.7±0.1*§	2.9±0.1	3.6±0.1‡
FS, %	31.7±1.7	23.5±1.9*§	31.2±1.5	25.6±2.3
Wall thickness, mm				
Infarct	N/A	0.70±0.03	N/A	0.61±0.02
Noninfarct	0.55±0.03	0.73±0.01†§	0.54±0.02	0.69±0.04*‡
Hemodynamic data				
LVSP, mmHg	100±3	68±2†	82±9*	69±2†
LV EDP, mmHg	4.8±0.4	6.0±0.5	4.4±0.7	5.8±0.5
+LV dP/dt_{max}, mm Hg/s	10 936±570	6433±545†‡	9200±1119	7133±492†
−LV dP/dt_{min}, mm Hg/s	10 836±784	6416±545†	9340±1386	7116±493†

Values are shown as mean±SEM. EDD indicates end-diastolic diameter; ESD, end-systolic diameter; FS, fractional shortening; N/A, not applicable; SP, systolic pressures; EDP, end-diastolic pressure; and dP/dt, maximum and minimal rate of pressure development.

*$P<0.5$, †$P<0.01$ vs sham-operated non-Tg mice.

‡$P<0.05$, §$P<0.01$ vs sham-operated BNP-Tg mice.

Results

Infarct Size, Echocardiography, and Hemodynamics

Three days after left coronary artery ligation, the sizes of the resultant infarcts were similar in BNP-Tg and non-Tg mice (BNP-Tg, 42.2±3.7% versus non-Tg, 40.4±3.8%; $P=0.75$, n=7). To evaluate the effect of a high plasma BNP concentration on the performance of the infarcted heart, we assessed cardiac function and LV geometry by use of echocardiography. The Table shows that the increase in LV chamber size and the noninfarcted wall thickness were the same in BNP-Tg and non-Tg mice 3 days after MI. LV systolic pressure measured by use of a Millar catheter was lower in sham-operated BNP-Tg mice than in sham-operated non-Tg mice (Table), which is consistent with our earlier observation that systolic blood pressure measured by use of the tail-cuff method was ≈20 mm Hg lower in BNP-Tg than non-Tg mice.[13] Conversely, there was no significant difference in LV systolic pressure, LV end-diastolic pressure, LV $+dP/dt_{max}$, or $-dP/dt_{min}$ between the 2 groups after ligation. We did, however, note a trend toward improved hemodynamic and echocardiographic parameters in BNP-Tg mice, although it did not reach statistical significance.

Infarct Infiltration by Neutrophils

Accumulation of leukocytes in the infarcted region is thought to be one step in the process of wound repair.[16,24] We therefore counted the leukocytes infiltrating the infarcted region after MI by use of a neutrophil-specific antibody. Neutrophils were identified throughout the infarcted segments after MI (Figure 1a). Moreover, although quantitative analysis of images of the infarcted region obtained 3 days after MI showed that their numbers increased in both BNP-Tg and non-Tg mice, there were significantly greater numbers of neutrophils in BNP-Tg than non-Tg hearts (BNP-Tg, 415.41±12.90 cells/mm^2 versus non-Tg, 330.70±16.82 cells/mm^2; $P<0.01$, n=6; Figure 1b).

To further assess neutrophil accumulation in the infarcted areas, we also measured MPO activity. As shown in Figure 1c, cardiac MPO activity was significantly higher in BNP-Tg than non-Tg mice 3 days after MI (BNP-Tg, 2.80±0.40 U/100 mg tissue versus non-Tg, 1.33±0.23 U/100 mg tissue; n=8 to 10, $P<0.01$), whereas there was no difference between the sham-operated groups.

Taken together, the data presented in this section clearly indicate that within 3 days after MI, neutrophils accumulate to a significantly greater degree in the infarcted regions of BNP-Tg hearts than non-Tg hearts.

Cardiac Gene Expression in Infarcted Hearts

Recent evidence highlights the involvement of the plasminogen activator–metalloproteinase system in myocardial neutrophil accumulation, the repair processes, and the rupture seen after MI.[15,16] When we examined gene expression of plasminogen activators and MMPs 3 days after MI, we found that, with the exception of GAPDH, transcription of all the genes examined was upregulated compared with sham-operated animals. In addition, expression of MMP-9 mRNA was significantly higher in BNP-Tg than non-Tg mice after ligation (Figure 2, a and b), whereas there was no difference in the expression of MMP-2, TIMP-1, urokinase-type plasminogen activator, and plasminogen activator inhibitor-1 mRNA in the 2 MI groups.

We also focused on the synthetic processes involved in collagen turnover by examining the expression of mRNAs encoding TGF-β_1, TGF-β_3, collagen I, and collagen III, which are known to be involved in cardiac fibroblast proliferation and the biosynthesis of ECM proteins.[25–27] We found that their expression was similarly upregulated in the infarcted regions of both BNP-Tg and non-Tg hearts (Figure 2, a and b), indicating that overexpression of BNP does not affect the biosynthesis of collagen during the early phase of acute MI.

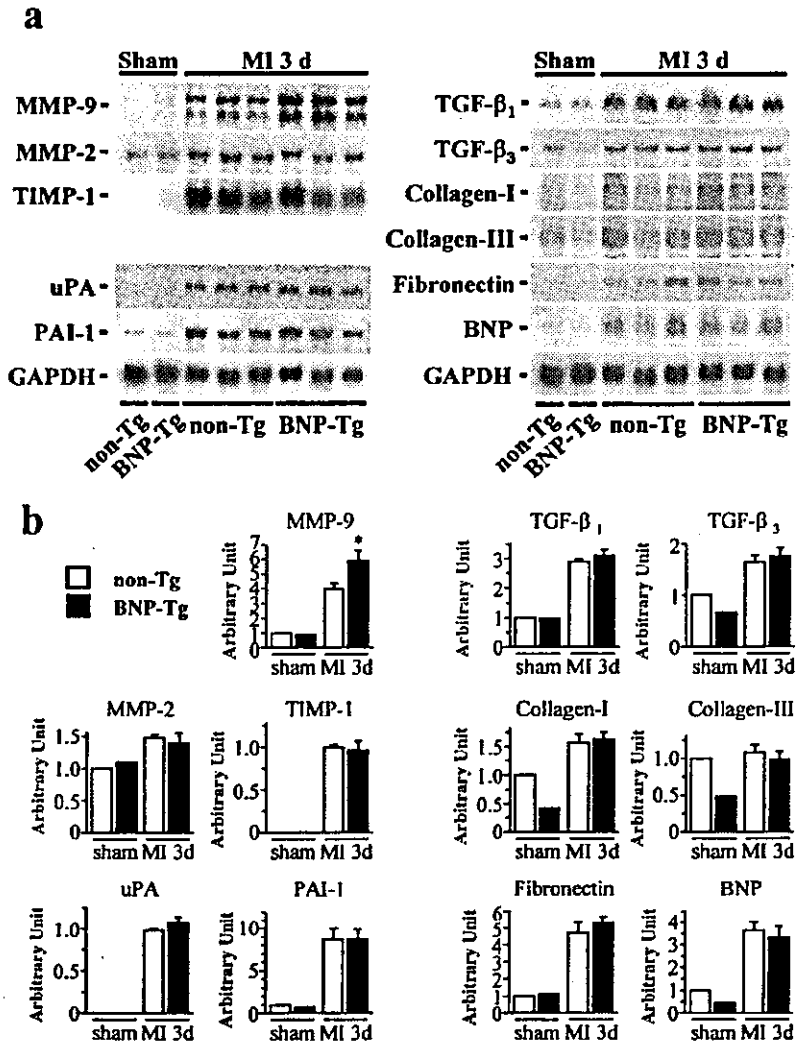

Figure 2. a, Representative autoradiograms showing Northern blot analysis in hearts harvested from sham-operated and infarcted mice 3 days after MI. b, Summary of results obtained from Northern blot analyses; mRNA levels in sham-operated non-Tg hearts were assigned a value of 1.0. Values are mean±SEM; *$P<0.05$ vs non-Tg mice with MI.

Increased MMP Activity in Infarcted Hearts

We next used gelatin zymography to evaluate the extent to which overexpression of BNP affects MMP-9 enzymatic activity. As shown in Figure 3a, the gelatinase activity of MMP-9, but not MMP-2, was significantly ($P<0.05$) elevated in infarcted BNP-Tg hearts compared with infarcted non-Tg hearts. Likewise, type IV collagenase activity was significantly higher in infarcted BNP-Tg than non-Tg hearts

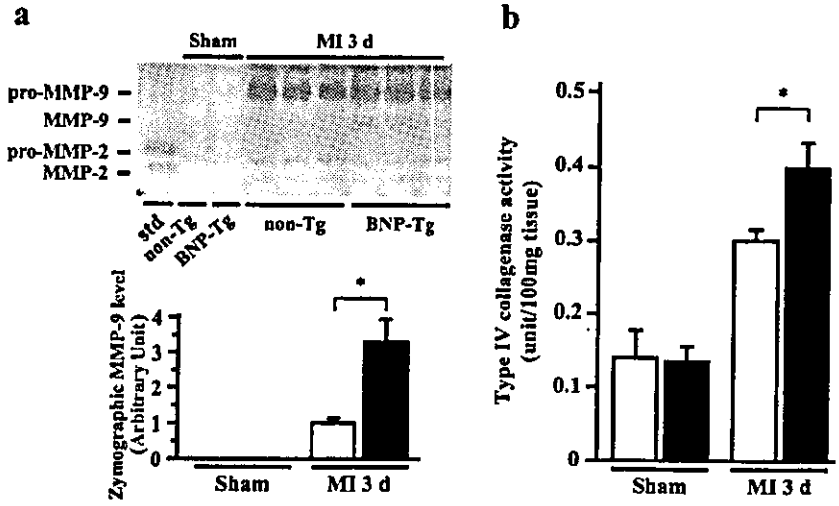

Figure 3. a, Top, Representative gelatin zymography performed 3 days after MI (n=6 for each); a mixture of human MMP-2 and pro-MMP-9 served as a standard (std). Bottom, densitometric analysis of MMP-9 abundance. b, Cardiac type IV collagenase activity expressed as units/100 mg tissue wet weight 3 days after MI (n=7 for each). Values are mean±SEM; *$P<0.05$ vs non-Tg mice with MI.

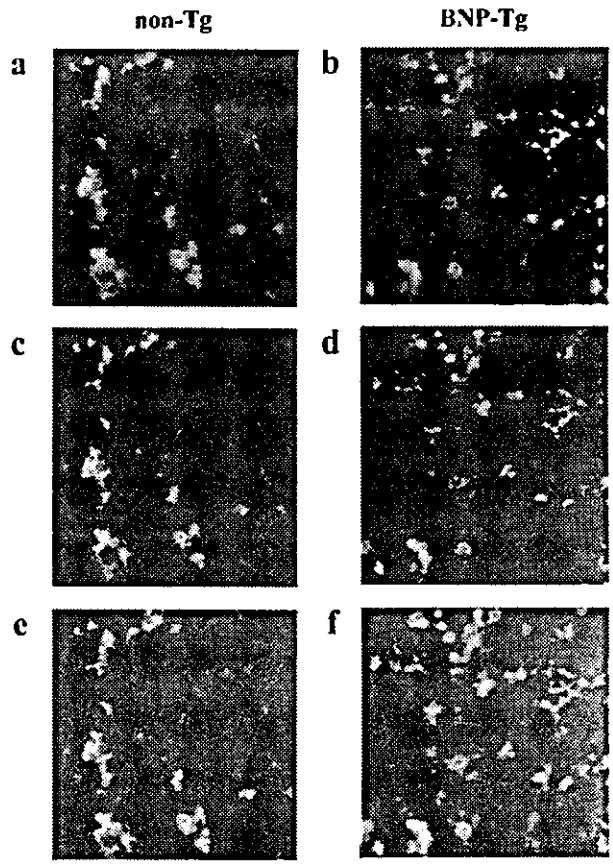

Figure 4. Confocal images of double immunostaining for MMP-9 and neutrophil 7/4. Immunostaining and cellular localization of MMP-9 within infarcted hearts of BNP-Tg (right) and non-Tg (left) mice 3 days after MI. Images show single immunostaining for MMP-9 (green) (a and b) and neutrophil 7/4 (red) (c and d). Double immunostaining (yellow) shows colocalization of MMP-9 within 7/4-stained neutrophils in infarcted region after MI (e and f). Magnification ×400.

(BNP-Tg, 0.399±0.037 U/100 mg wet wt versus non-Tg, 0.300±0.017 U/100 mg wet wt; n=7, $P<0.05$; Figure 3b). Because MMP-9 and -2 are the 2 major collagenases that degrade type IV collagen[23] and zymography showed that there was no difference in MMP-2 activity within the infarcts of BNP-Tg and non-Tg mice, the increased digestion of type IV collagen in BNP-Tg hearts is attributable to the increase in MMP-9 activity.

Neutrophils Are the Predominant Source of MMP-9

We then evaluated the distribution of the MMP-9 by using confocal fluorescence microscopy to visualize the double immunostaining of MMP-9 (green) and neutrophils (red) in thin sections of frozen mouse LV. Three days after MI, immunoreactive MMP-9 and neutrophils were detected within the infarcted myocardium and the border regions in both BNP-Tg and non-Tg hearts (Figure 4, a–d). Moreover, the double labeling revealed that the distribution of immunoreactive neutrophils overlapped that of MMP-9 (Figure 4, e and f), indicating that the major source of MMP-9 is the neutrophils infiltrating the infarcted region. By contrast, MMP-9 levels were negligible in the sham-operated mice and the noninfarcted regions of the infarcted mice (data not shown).

MMP-9 Inhibition Did Not Affect Neutrophil Infiltration in BNP-Tg

Finally, we assessed the functional significance of MMPs in BNP-Tg mice subjected to experimental MI by treating the mice with doxycycline, a nonselective MMP inhibitor. We found that the numbers of neutrophils detected by use of anti-mouse neutrophil 7/4 antibody were similarly increased in control BNP-Tg and doxycycline-treated BNP-Tg mice (control BNP-Tg, 428.24±29.84 cells/mm^2 versus doxycycline-treated BNP-Tg, 432.93±23.86 cells/mm^2; $P=0.90$, n=6; Figure 5, a and b). Likewise, there were no significant differences in the cardiac MPO activity in control BNP-Tg and doxycycline-treated BNP-Tg mice (control BNP-Tg, 3.03±0.36 U/100 mg tissue versus doxycycline-treated BNP-Tg, 2.80±0.32 U/100 mg tissue; $P=0.63$; Figure 5c). Thus, the increased infiltration of neutrophils into the infarcted area was not dependent on increased MMP-9 activity in the neutrophils themselves.

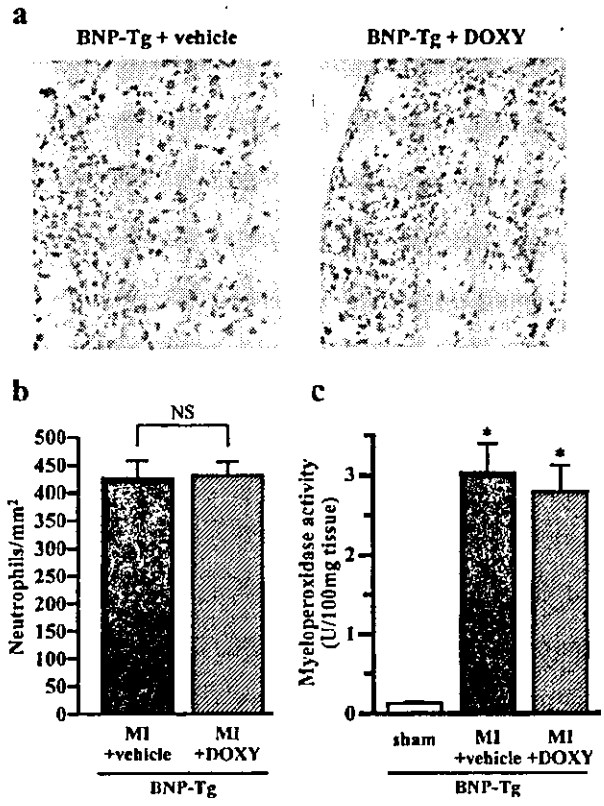

Figure 5. Accumulation of neutrophils within infarcted regions of control BNP-Tg and doxycycline-treated BNP-Tg mice. a, Representative micrograph showing stained neutrophils within infarct area (magnification ×200). b, Numbers of neutrophils per mm^2 within infarcted area 3 days after MI (n=6 for each). Values are shown as mean±SEM; NS, not significant. c, Cardiac MPO activity expressed as units/100 mg tissue wet weight in sham-operated (n=3 for each), untreated infarcted (n=18), and doxycycline-treated infarcted BNP-Tg mice (n=17). Values are mean±SEM; *$P<0.01$ vs sham values.

Discussion

We previously showed that plasma BNP levels are greatly elevated in patients with acute MI; they reach a peak within 24 hours after onset, then decline and increase again to a second peak over the next 3 to 7 days.[5] Thus, high plasma BNP levels persist during the period when neutrophils and other inflammatory cells infiltrate the infarcted area. In the present study, we used BNP-Tg mice to assess the effects of a pharmacological dose of BNP on the myocardium early after acute MI. We found that (1) there is a greater accumulation of neutrophils in BNP-Tg hearts; (2) gene expression and enzyme activity of MMP-9 are higher in BNP-Tg hearts; (3) the major source of MMP-9 is the neutrophils infiltrating the infarcted region of BNP-Tg hearts; and (4) doxycycline, a potent MMP inhibitor, has no effect on the increased infiltration of neutrophils into the infarcted area in BNP-Tg mice.

The wound repair process involves temporally overlapping phases that include inflammation, new tissue formation, and tissue remodeling.[28] During the inflammatory phase, collagen and other ECM components may be degraded as a result of increased MMP activity.[29,30] In the present study, we found that early after MI, neutrophil infiltration of the infarcted area is augmented in BNP-Tg mice, and that there are corresponding increases in MMP-9 expression and activity associated with the infiltrating neutrophils. By contrast, there were no significant changes in the levels of TGF-β_1, TGF-β_3, collagen I, collagen III, or fibronectin mRNA, which suggests that overexpression of BNP leads to exaggerated collagen degradation by MMP-9 produced by neutrophils without an apparent increase in synthesis. Moreover, the fact that the increase in zymographic MMP-9 activity in BNP-Tg mice appeared to be more pronounced than the increase in neutrophil number suggests that BNP may have a direct effect on the amount of MMP-9 activity produced by each activated neutrophil. This idea is supported by the results of supplemental experiments showing that in the presence of the neutrophil-activating factor formyl-methionyl-leucyl-phenylalanine (fMLP; 10^{-7} mol/L), ANP (10^{-8} mol/L), which shares its receptor (NPRA) with BNP and is equally potent, elicited a 2.1-fold increase ($P<0.01$) in the transcription and activation of MMP-9 in human neutrophils.

We also tested whether upregulation of MMP-9 contributes to the accumulation of neutrophils in BNP-Tg mice. On the basis of evidence that it suppresses the activity of such MMPs as collagenase, gelatinase, and stromelysin both directly and indirectly,[31] we used doxycycline to evaluate the extent to which elevated MMP production is involved in neutrophil accumulation within the infarcted regions of BNP-Tg hearts. That we found no difference in the neutrophil accumulation in control BNP-Tg and doxycycline-treated BNP-Tg mice suggests that the increased MMP-9 activity is most likely not responsible for the neutrophil accumulation in BNP-Tg animals. Conversely, one possible explanation for the increased leukocyte infiltration is that BNP exerts a direct effect on neutrophil chemotaxis. In fact, a recent study has shown that ANP affects human neutrophil migration at concentrations ranging from 4×10^{-9} to 10^{-7} mol/L.[32] The plasma BNP concentration in BNP-Tg mice was approximately 3×10^{-9} mol/L, which is comparable to the effective ANP concentration reported earlier, because ANP and BNP act via NPRA with equal potency. Another possible explanation is an indirect effect via endothelial adhesion molecules. We previously showed that the diminished neutrophil accumulation seen during ischemia/reperfusion in NPRA-deficient mice is probably a result of suppressed expression of P-selectin in coronary endothelial cells and that ANP upregulates P-selectin expression in cultured endothelial cells exposed to oxidative stress.[20] Thus, BNP might increase neutrophil accumulation by upregulating one or more of the endothelial adhesion molecules that tether circulating neutrophils to the endothelium.

Heymans et al[16] recently showed that MMP-9 deficiency retards the wound healing process after MI in mice, which increases the size of residual necrotic areas. In the same study, these investigators also showed that the lack of MMP-9 proteolytic activity results in almost complete protection against infarct rupture. These results suggest that MMP-9 is a key regulator of infarct healing and rupture, acting via degradation of ECM early after acute MI. Indeed, BNP-Tg mice tended to die of cardiac rupture more frequently than non-Tg mice: among the dead mice (26 BNP-Tg and 9 non-Tg), 47.1% (n=24) of the BNP-Tg mice died of cardiac rupture after MI, whereas 18.6% (n=2) of non-Tg mice died of the same cause ($P=0.75$ by χ^2 analysis). Moreover, although the effect did not reach statistical significance, doxycycline tended to attenuate cardiac rupture in BNP-Tg mice, suggesting that elevated MMP-9 activity may be involved. However, because the level of collagen and TGF-β expression is lower in sham-operated BNP-Tg hearts than in sham-operated non-Tg hearts (Figure 2), the apparent high frequency of cardiac rupture in BNP-Tg mice might be attributable to a reduction in collagen matrix in BNP-Tg mice. More importantly, the transient activation of MMP-9 induced by BNP may speed up infarct healing and modulate the overall late remodeling process. In fact, at 6 weeks after ligation, LV dilatation and hypertrophy of the noninfarcted zone seen in the non-Tg mice are attenuated in BNP-Tg mice (our unpublished data). These observations suggest that transient MMP-9 expression induced by the elevation in BNP during the earliest phase after MI is a cardioprotective mechanism affecting late LV remodeling.

In summary, overexpression of BNP in mice led to neutrophil infiltration and MMP-9 expression in the infarcted region after MI, an effect that could lead to exaggerated degradation of ECM components. This suggests that BNP plays a novel role in the process of cardiac repair during the acute phase of MI.

Acknowledgments

This work was supported in part by research grants from the Japanese Ministry of Education, Science, and Culture; the Japanese Ministry of Health and Welfare; and the Japanese Society for the Promotion of Science Research for the Future program (JSPS-RFTF96I00204 and JSPS-RFTF98L00801). Excellent secretarial work by K. Okamura is also acknowledged.

References

1. De Bold AJ. Atrial natriuretic factor: a hormone produced by the heart. *Science.* 1985;230:767–770.

2. Rosenzweig A, Seidman CE. Atrial natriuretic factor and related peptide hormones. *Annu Rev Biochem.* 1991;60:229–255.
3. Mukoyama M, Nakao K, Hosoda K, et al. Brain natriuretic peptide as a novel cardiac hormone in humans: evidence for an exquisite dual natriuretic peptide system, atrial natriuretic peptide and brain natriuretic peptide. *J Clin Invest.* 1991;87:1402–1412.
4. Mukoyama M, Nakao K, Saito Y, et al. Increased human brain natriuretic peptide in congestive heart failure. *N Engl J Med.* 1990;323:757–758.
5. Morita E, Yasue H, Yoshimura M, et al. Increased plasma levels of brain natriuretic peptide in patients with acute myocardial infarction. *Circulation.* 1993;88:82–91.
6. Yamamoto K, Burnett JC Jr, Jougasaki M, et al. Superiority of brain natriuretic peptide as a hormonal marker of ventricular systolic and diastolic dysfunction and ventricular hypertrophy. *Hypertension.* 1996; 28:988–994.
7. Nagaya N, Goto Y, Nishikimi T, et al. Sustained elevation of plasma brain natriuretic peptide levels associated with progressive ventricular remodelling after acute myocardial infarction. *Clin Sci.* 1999;96: 129–136.
8. Tamura N, Ogawa Y, Chusho H, et al. Cardiac fibrosis in mice lacking brain natriuretic peptide. *Proc Natl Acad Sci U S A.* 2000;97:4239–4244.
9. Mills RM, LeJemtel TH, Horton DP, et al. Sustained hemodynamic effects of an infusion of nesiritide (human b-type natriuretic peptide) in heart failure: a randomized, double-blind, placebo-controlled clinical trial. Natrecor Study Group. *J Am Coll Cardiol.* 1999;34:155–162.
10. Colucci WS, Elkayam U, Horton DP, et al. Intravenous nesiritide, a natriuretic peptide, in the treatment of decompensated congestive heart failure. Nesiritide Study Group. *N Engl J Med.* 2000;343:246–253.
11. Holtwick R, van Eickels M, Skryabin BV, et al. Pressure-independent cardiac hypertrophy in mice with cardiomyocyte-restricted inactivation of the atrial natriuretic peptide receptor guanylyl cyclase-A. *J Clin Invest.* 2003;111:1399–1407.
12. Molkentin J. A friend within the heart: natriuretic peptide receptor signaling. *J Clin Invest.* 2003;111:1275–1277.
13. Ogawa Y, Itoh H, Tamura N, et al. Molecular cloning of the complementary DNA and gene that encode mouse brain natriuretic peptide and generation of transgenic mice that overexpress the brain natriuretic peptide gene. *J Clin Invest.* 1994;93:1911–1921.
14. Chusho H, Ogawa Y, Tamura N, et al. Genetic models reveal that brain natriuretic peptide can signal through different tissue-specific receptor-mediated pathways. *Endocrinology.* 2000;141:3807–3813.
15. Creemers E, Cleutjens J, Smits J, et al. Disruption of the plasminogen gene in mice abolishes wound healing after myocardial infarction. *Am J Pathol.* 2000;156:1865–1873.
16. Heymans S, Luttun A, Nuyens D, et al. Inhibition of plasminogen activators or matrix metalloproteinases prevents cardiac rupture but impairs therapeutic angiogenesis and causes cardiac failure. *Nat Med.* 1999;5: 1135–1142.
17. Michael LH, Entman ML, Hartley CJ, et al. Myocardial ischemia and reperfusion: a murine model. *Am J Physiol.* 1995;269:H2147–H2154.
18. Patten RD, Aronovitz MJ, Deras-Mejia L, et al. Ventricular remodeling in a mouse model of myocardial infarction. *Am J Physiol.* 1998;274: H1812–H1820.
19. Ichihara S, Senbonmatsu T, Price E Jr, et al. Targeted deletion of angiotensin II type 2 receptor caused cardiac rupture after acute myocardial infarction. *Circulation.* 2002;106:2244–2249.
20. Izumi T, Saito Y, Kishimoto I, et al. Blockade of the natriuretic peptide receptor guanylyl cyclase-A inhibits NF-kappaB activation and alleviates myocardial ischemia/reperfusion injury. *J Clin Invest.* 2001;108: 203–213.
21. Silvestre JS, Mallat Z, Tamarat R, et al. Regulation of matrix metalloproteinase activity in ischemic tissue by interleukin-10: role in ischemia-induced angiogenesis. *Circ Res.* 2001;89:259–264.
22. Cho A, Reidy MA. Matrix metalloproteinase-9 is necessary for the regulation of smooth muscle cell replication and migration after arterial injury. *Circ Res.* 2002;91:845–851.
23. Fujimura M, Gasche Y, Morita-Fujimura Y, et al. Early appearance of activated matrix metalloproteinase-9 and blood-brain barrier disruption in mice after focal cerebral ischemia and reperfusion. *Brain Res.* 1999;842: 92–100.
24. Jugdutt BI. Ventricular remodeling after infarction and the extracellular collagen matrix: when is enough enough? *Circulation.* 2003;108: 1395–1403.
25. Weber KT, Brilla CG. Pathological hypertrophy and cardiac interstitium: fibrosis and renin- angiotensin-aldosterone system. *Circulation.* 1991;83: 1849–1865.
26. Butt RP, Laurent GJ, Bishop JE. Mechanical load and polypeptide growth factors stimulate cardiac fibroblast activity. *Ann N Y Acad Sci.* 1995;752: 387–393.
27. Cleutjens JP, Verluyten MJ, Smiths JF, et al. Collagen remodeling after myocardial infarction in the rat heart. *Am J Pathol.* 1995;147:325–338.
28. Singer AJ, Clark RA. Cutaneous wound healing. *N Engl J Med.* 1999; 341:738–746.
29. Etoh T, Joffs C, Deschamps A, et al. Myocardial and interstitial matrix metalloproteinase activity after acute myocardial infarction in pigs. *Am J Physiol.* 2001;281:H987–H994.
30. Tao ZY, Cavasin MA, Yang F, et al. Temporal changes in matrix metalloproteinase expression and inflammatory response associated with cardiac rupture after myocardial infarction in mice. *Life Sci.* 2004;74: 1561–1572.
31. Golub LM, Lee HM, Ryan ME, et al. Tetracyclines inhibit connective tissue breakdown by multiple non-antimicrobial mechanisms. *Adv Dent Res.* 1998;12:12–26.
32. Elferink JG, De Koster BM. Atrial natriuretic factor stimulates migration by human neutrophils. *Eur J Pharmacol.* 1995;288:335–340.

Complementary antagonistic actions between C-Type natriuretic peptide and the MAPK pathway through FGFR-3 in ATDC5 Cells

Ami Ozasa[a], Yasato Komatsu[a], Akihiro Yasoda[a], Masako Miura[a], Yoko Sakuma[a], Yuko Nakatsuru[a], Hiroshi Arai[a], Nobuyuki Itoh[b] and Kazuwa Nakao[a]

[a]Department of Medicine and Clinical Science, Kyoto University Graduate School of Medicine

[b]Department of Genetic Biochemistry, Kyoto University Graduate School of Pharmaceutical Sciences

Corresponding and reprint requests to: Yasato Komatsu, M.D., Ph.D.

Department of Medicine and Clinical Science, Kyoto University Graduate School of Medicine. 54 Shogoin Kawahara-cho Sakyo-ku, Kyoto 606-8507, Japan

Phone:81-75-751-3181; fax:81-75-771-9452 :komatsuy@barium.rirc.kyoto-u.ac.jp

Key words: natiuretic peptide, gyanylyl cyclase, chondrocyte, FGF, MAPK

ABSTRACT

We previously reported that C-type natriuretic peptide (CNP) stimulates endochondral ossification and corrects the reduction in body length of achondroplasia model mouse with constitutive active fibroblast growth factor receptor 3 (FGFR-3). In order to examine the interaction between CNP and FGFR-3, we studied intracellular signaling by using ATDC5 cells, a mouse chondrogenic cell line, and found that FGF2 and FGF18 markedly reduced CNP-dependent intracellular cGMP production, and that these effects were attenuated by MAPK inhibitors. Western blot analysis demonstrated that the level of GC-B, a particulate guanylyl cyclase specific for CNP, was not changed by treatment with FGFs. Conversely, CNP and 8-bromo-cGMP strongly and dose-dependently inhibited the induction of ERK phosphorylation by FGF2 and FGF18 without changing the level of FGFR-3, although they did not affect the phosphorylation of STAT-1. In the organ cultured fetal mouse tibias, CNP and FGF18 counteracted on the longitudinal bone growth, and both the size and number of hypertrophic chondrocytes. The FGF/FGFR-3 pathway is known as the negative regulator of endochondral ossification. We found that FGFs inhibited CNP-stimulated

cGMP production by disrupting the signaling pathway through GC-B while CNP antagonized the activation of the MAPK cascade by FGFs. These results suggest that the CNP/GC-B pathway plays an important role in growth plate chondrocytes and constitutes the negative cross talk between FGFs and the activity of MAPK. Our results may explain one of the molecular mechanisms of the growth stimulating action of CNP and suggest that activation of the CNP/GC-B pathway may be effective as a novel therapeutic strategy for achondroplasia.

INTRODUCTION

The natriuretic peptide family consists of three structurally related peptides: atrial natriuretic peptide (ANP), brain natriuretic peptide (BNP) and C-type natriuretic peptide (CNP) (1). They can influence a variety of homeostatic processes by accumulation of the intracellular guanosine 3', 5'-cyclic monophosphate (cGMP) through two subtypes of particulate guanylyl cyclase (GC), GC-A for ANP and BNP, and GC-B for CNP (2). In skeletal tissues, we have demonstrated that CNP is a positive growth regulator of long bones formed through endochondral ossification via the GC-B/cGMP pathway (3, 4). CNP-depleted mice are characterized by short stature with a phenotype histologically similar that of achondroplasia (3), while the growth plates of explanted long bones in the presence of CNP show a similar histological picture to that of the growth plate cartilage of fibroblast growth factor receptor 3 (FGFR-3)-depleted mice (5). This raises the possibility that activation of the CNP/GC-B pathway of endochondral bone regulation reverses the inhibitory effect of FGFR-3 signaling in skeletogenesis.

FGFR-3 belongs to a class of tyrosine kinase receptors involved in signal

transduction. In the presence of soluble or cell-surface heparin sulfate proteoglycans, fibroblast growth factors (FGFs) binding to FGFRs induce receptor dimerization and autophosphorylation on tyrosine residues. This then triggers cell proliferation or differentiation through the Ras-Raf-dependent and phospholipase C-dependent signal transduction pathways involving MAPK stimulation (6). FGFR-3 mutations have been shown to be responsible for achondroplasia, hypochondroplasia and thanatophoric dysphasia (TDI and TDII) (7, 8). These mutations activate receptor signaling by either inducing ligand-independent receptor dimerization or easing the constraints on autophosphorylation of receptor-tyrosine kinase (9). It has recently been reported that, of the 23 members of the FGF family, FGF-18 is a physiologic ligand for FGFR-3 in chondrocytes, and plays an important role as a mediator in skeletal development (10, 11, 12).

To gain further insight into the cellular basis of the interaction between CNP and FGFs in endochondral bone formation, we used ATDC5 cells, which constitute a mouse chondrogenic cell line derived from embryogenic carcinoma cells (13). In the presence of insulin, these cells differentiate into chondrocytes, form cartilage nodules,

serially exhibit several differentiation markers for the chondrocytes, and are eventually mineralized, thus reflecting the endochondral ossification process *in vivo*. We previously demonstrated that ATDC5 cells contain particularly high activity levels for GC-B and also appear to contain low levels of GC-A and the soluble form of guanylyl cyclase, which is responsive to nitric oxide (14). Therefore, ATDC5 cells are considered to be a good model to study the interaction between CNP and FGFs *in vitro*.

We also studied the effects of CNP and FGF18 on organ-cultured fetal mouse tibias. Since the growth plates consist of several zones, each representing a different stage of differentiation and functioning differently, the interaction between the cells in the different zones can be crucial for a given substance to exert its effects. We previously developed an *ex vivo* organ culture system of mouse long bones (4). During a 5-day culture, the bones exhibited longitudinal growth mostly due to the growth in the cartilage primordial rather than the ossified portion. This system was therefore considered a good *ex vivo* model for studying the interaction between CNP and FGFs. The purpose of the study presented here was to clarify the interaction between the CNP/GC-B pathway and FGF signaling in growth plate chondrocytes, as well as the

mechanism of this interaction, in order to determine the efficacy of activation of CNP/GC-B as a novel therapeutic strategy for achondroplasia.

Materials and Methods

Human C-type natriuretic peptide was purchased from Peptide Institute, Inc. (Minoh, Japan), 8-bromo cGMP and isobutylmethylxanthine (IBMX) from Sigma-Aldrich Co. (St.Louis, MO, USA), and human recombinant FGF2 from Pepro Tech EC.Ltd. (London, England). Rat recombinant FGF18 was generously provided by Amgen Inc. (Thousand Oaks, CA, USA). Primary antibodies, rabbit anti-phospho-ERK1/2 antibodies, rabbit anti- ERK1/2 antibodies, and anti-STAT-1 antibodies were obtained from Cell Signaling Technology Inc. (Beverly, MA, USA), rabbit anti-phospho-STAT-1 antibodies from Upstate Biotechnology, (Lake Placid, NY, USA), and HRP-conjugated donkey anti-rabbit IgG antibodies from Amersham Pharmacia Biotech, (Freiburg, Germany). The MEK (MAPK- ERK kinase) inhibitors U0126 and PD098059 were purchased from Cell Signaling Technology Inc., fetal calf serum (FCS) was purchased from Sankou Junyaku (Tokyo, Japan), and Ham F12/DMEM 50/50 medium and Bigger's BJG medium were obtained from GIBCO (Grand Island, NY, USA).

Cell culture conditions

Cells were grown and maintained using standard techniques. ATDC5 cells were maintained in Ham F12/DMEM 50/50 medium containing 5% FCS, antibiotics and insulin (10ng/ml). Confluent cells were maintained for 14 days, and considered quiescent after maintenance in 0.5%FCS for 24h. For radioimmunoassay, cells were seeded on 24-multiwell culture plates, and on a 6cm dish (BD Bioscience, NJ, USA) for Western blotting and real-time PCR analysis.

Intracellular cGMP determination

Quiescent cells were treated with FGFs for one hour. The cells were then preincubated in Ham F12/DMEM 50/50 medium containing 0.5% FCS and 1mM IBMX at room temperature for 10min. CNP was added at a concentration of 10^{-9}~10^{-7}M and incubated at 37°C for 30min in the presence of 1mM IBMX. Reactions were terminated immediately by aspirating the medium, washing the cells with ice-cold PBS, and freezing them in 500μl of 50mM HCl. The acidified extracts were analyzed for guanylyl cyclase activity. The level of cGMP was determined by radioimmunoassay after succinylation (Yamasa Co. Ltd., Chosi, Chiba, Japan). To examine the effect of FGFs, we also used the MEK inhibitors U0126 and PD098059, which were added one

hour before treatment of CNP. The level of cGMP was determined as already described.

Western blot analysis

Quiescent cells were incubated with a medium containing CNP (10^{-7}~10^{-6}M) or 10^{-4}M 8-bromo cGMP for one hour. The medium was then switched to an FGF-containing one, and the cells were treated with FGFs (10ng/ml) for 3min. Cells were extracted with the aid of a solvent solution (0.5M Tris-HCl, 10%SDS, β-mercaptethanol, glycerol, and Bromo-phenol blue). Soluble proteins were electrophoretically resolved on 8% acrylamide, 0.1% SDS gels and transferred to polyvinylidene fluoride membranes (Immobilon-P; Millipore, Billerica, MA, USA). The membranes were probed overnight with antibodies against phosphorylated ERK1/2, ERK1/2, phosphorylated STAT-1 or STAT-1, according to the supplier's instructions. The membranes were then probed with secondary antibodies for 1 hour. Bound antibodies were detected by chemiluminescence (ECL, Amersham Pharmacia Biotech, Piscataway, NJ, USA) and their density measured by using the public domain National Institute of Health IMAGE program.

The expression of GC-B in ATDC5 cells was analyzed by Western blot analysis.

Quiescent cells were incubated with a medium containing FGF18 (1 or 10ng/ml) for one hour, after which the cells were extracted and the proteins blotted to the membrane as described above. The membranes were probed for one hour with the rabbit polyclonal anti-GC-B antibody (15) (a generous gift from Dr. D.L. Garbers of the University of Texas Southwestern Medical Center) and bound antibodies were detected as described above.

To confirm the effect of the MEK inhibitor on phosphorylated ERK1/2, we used 20μM U0126, and the MEK inhibitor (U0126) was added one hour before treatment of FGF2.

Real-time PCR analysis of FGFR-3

Quiescent cells were incubated with a medium containing CNP (10^{-6}M) for one hour and total RNAs were extracted using ISOGEN (Nippon Gene Co. Ltd., Toyama, Japan) according to the manufacturer's instructions. After synthesis of the first-strand cDNA from 1 μg of total RNA by means of Superscript II RT (Life Technologies, Inc., St. Louis, MO, USA) with random hexamers, Taqman-PCR was performed with the ABI Prism 7700 sequence detection system and Taqman Universal

PCR Mastermix (Applied Biosystems, Foster City, CA, USA) using FAM and VIC-labeled fluorogenic probes specific for FGFR-3 or the internal standard 18S rRNA. All samples were run in duplicate in 96-well plates in the ABI Prism 7700 sequence. There was no significant difference in 18S rRNA levels among experimental groups.

Organ culture of embryonic mouse tibias

Organ culture of fetal mouse tibias was performed with the suspension culture technique in a chemically defined medium (Bigger's BJG medium). Tibial explants from 16-day-old normal ICR mouse embryos were cultured for 5 days with or without 10ng/ml FGF18 and 10^{-7}M CNP. After a 5-day culture, the total bone length was measured longitudinally by using a linear ocular scale mounted on an inverted microscope. Explants were fixed in 4% paraformaldehyde, decalcified in 10% EDTA/ 0.1M Tris-HCl, pH 7.4, for 7 days, and embedded in paraffin. 5μm -thick sections cut from the paraffin-embedded specimens were stained with Alcian blue (PH2.5) and hematoxylin/eosin (H&E).

Immunohistochemical staining for type X collagen, using a polyclonal rabbit anti-type X collagen antibody (1:5000; LSL, Tokyo, Japan) as a primary antibody, was

also performed. Immunoreactions were visualized by using a biotinylated antipolyvalent antibody, a streptavidin-biotin-horseradish peroxidase complex, and diaminobenzidine (Vector Laboratories, Inc., Burlingame, CA, USA). The specificity of the immunoreactions was controlled by omitting the primary antibody.

The size of hypertrophic cells was measured on 5μm-thick sections of cultured tibias with a computerized measurement system (KS400 Imaging System; Carl Zeiss, Eching, Germany), and the cells of hypertrophic chondrocytes were manually counted.

Statistical analysis

Data are expressed as the mean±SE. The changes in cGMP were compared by means of ANOVA using Fisher's test. Comparisons between groups of organ cultured bone lengths were performed with the unpaired t test. Probabilities less than 0.05 were considered statistically significant.

RESULTS

Inhibition by FGF2 of CNP signaling in ATDC5 cells

ATDC5 cells were differentiated into chondrocytes for a 14-day culture after confluency (13), and we confirmed that collagen type X, a marker of hypertrophic chondrocytes, was expressed in these cells (16). In ATDC5 cells, CNP (10^{-9}-10^{-7}M) stimulated the production of intracellular cGMP in a dose-dependent manner with a 36-fold increase of the basal level at 10^{-7}M CNP (55±3fmol/ well to 1985±181fmol/ well). This increase was inhibited up to 53% by the addition of 10ng/ml of FGF 2 (1045±65fmol/ well) (Fig.1 A). Pretreatment with U0126, a specific inhibitor of the upstream of ERK (MEK) (17), at a concentration of 20μM partially undid the reduction of cGMP by FGF2 (1395±144fmol/ well vs. 1980±143fmol/ well) compared with the vehicle (Fig.1 B). The same level of recovery was observed after pretreatment with another MEK inhibitor, PD098059, also at a concentration of 20μM (1425±276fmol/ well vs. 1620±206fmol/ well). Western blot analysis was performed to confirm the blockade of U0126 to ERK1/2 phosphorylation by FGF2. Pretreatment with 20μM U0126 completely blocked the phosphorylation of ERK1/2 (Fig.1 B *inset*).

Inhibition by FGF18 of CNP signaling in ATDC5 cells

We analyzed the effect of FGF18, the specific ligand for FGFR-3 in chondrocytes, on CNP-dependent cGMP production in ATDC5 cells. As in the case of FGF2, FGF18 inhibited intracellular cGMP production in ATDC5 cells in a dose dependent manner (0.3-100ng/ml). Preincubation with 3ng/ml FGF18 significantly inhibited the increase in 10^{-7}M CNP stimulated cGMP production (1425±82fmol/ well vs. 1975±111fmol/ well). This inhibition by FGF18 reached 64% at a concentration of 10ng/ml and 100ng/ml FGF18 (1255±11fmol/ well) (Fig.2).

No effect of FGF18 on GC-B expression in ATDC5 cells

To confirm the expression level of GC-B, the specific receptor for CNP in ATDC5 cells, we performed Western blot analysis using antiserum specific for GC-B. The quiescent ATDC5 cells expressed a certain amount of GC-B at 120-kDa band, which incubation with FGF18 (1 or 10ng/ml) for 1 hour did not alter (Fig.2 *inset*).

Attenuation by CNP of MAPK activity of FGFs

The effect of CNP on the downstream signaling of FGFR-3 in ATDC5 cells was analyzed next. ERK1/2 phosphorylation was barely detectable at the basal level but